Catalysis Today 227 (2014) 215–222

Contents lists available at ScienceDirect

Catalysis Today

journal homepage: www.elsevier.com/locate/cattod

# Amino-grafted SBA-15 material as dual acid–base catalyst for the synthesis of coumarin derivatives

Nadia Aider[a,b,c], Agata Smuszkiewicz[a], Elena Pérez-Mayoral[a,*], Elena Soriano[d], Rosa M. Martín-Aranda[a], Djamila Halliche[b], Saliha Menad[b,c]

[a] Departamento de Química Inorgánica y Química Técnica, Facultad de Ciencias, Universidad Nacional de Educación a Distancia, UNED, Paseo Senda del Rey 9, E-28040 Madrid, Spain
[b] Laboratoire Gaz Naturel, University of Sciences and Technology Houari Boumediene (USTHB), Argel, Algeria
[c] Département de chimie, Faculté des Sciences (UMMTO), Tizi-ouzou, Algeria
[d] Instituto de Química Orgánica General (CSIC), C/Juan de la Cierva 3, 28006 Madrid, Spain

ARTICLE INFO

*Article history:*
Received 5 July 2013
Received in revised form 2 October 2013
Accepted 4 October 2013
Available online 31 October 2013

*Keywords:*
Mesoporous materials
Heterogeneous catalysis
Coumarins
Knoevenagel condensation
Computational methods

ABSTRACT

We report herein an experimental and theoretical study concerning the preparation of the coumarins (**2**) from 2-hydroxybenzaldehydes (**3**) and ethyl acetoacetate (**4**) promoted by amino-grafted SBA-15 materials. The reaction takes places by Knoevenagel condensation between reagents, in the absence of any solvent and under mild conditions, followed by a non catalytic lactonization step.

Amino-grafted SBA-15 loaded with secondary amine groups, MAP/SBA-15, was found to be the most efficient and totally recyclable catalyst as compared with its analog containing tertiary amine groups, DEAP/SBA-15 (where MAP and DEA are methyl aminopropyl and diethyl aminopropyl groups, respectively). Our theoretical analysis confirms that the steric congestion and the absence of —NH protons as the catalytic active sites are determining factors for the increasing of the activation barrier and, therefore, for the lower catalytic activity and reactivity to the formation of the coumarin.

The computational study herein reported demonstrates that MAP/SBA-15, a traditional basic mesoporous silica having —NH protons, shows a dual acid–base catalytic behavior when used in the synthesis of coumarins via Knoevenagel condensation.

Otherwise, the substitution in 2-hydroxybenzaldehydes (**3**) at 5-position clearly influences the acceptor and acidity capacities of the —CHO and the —OH groups as experimentally and theoretically demonstrated.



## 1. Introduction

The research on ordered mesoporous silicas has undergone an impressive progress since the discovery of MCM-41 by Scientifics of Mobil Corporation in 1992 [1]. In fact the development of new modified mesoporous silicas is an area of extensive research constituting a hot issue of current interest in nanochemistry.

In general, the main and useful property of the ordered mesoporous silicas is their large specific surface area; their walls can be tuned by the introduction of high concentrations of active functions which allow their application for adsorption and catalysis [2].

Mesoporous silicas have been extensively studied for capture and separation of gases; particularly basic ordered mesoporous materials functionalized with amine groups, by using different synthetic methods or by impregnation [3,4], are highly selective materials to adsorption of carbon dioxide. Pore volume of the silica matrix is an important factor which determines the $CO_2$ adsorption capability of the amine-loaded. In this sense, ordered mesoporous amino grafted MCM-48 [5,6], pore-expanded amino-grafted MCM-41 [7] SBA-15 [8–10] or even MCF materials [11] have been developed and tested for $CO_2$ capture.

Likewise, amino-containing mesoporous silicas also found application in catalysis. Our research group possesses a wide experience in this field involving the mesoporous silicas functionalized with aminopropyl groups in the preparation of heterocyclic compounds with synthetic interest; thus, amino-grafted MCM-41 materials are able to catalyze the selective *N*-alkylation of pyrazole [12] whereas amino-grafted metallosilicate MCM-41 efficiently promote the isomerization of Safrole [13], the Knoevenagel condensation [14] and the synthesis of *N*-alkyl imidazoles under ultrasound activation [15].

On other hand, the knowledge of these processes faces with the difficulty in getting accurate structural information on these amorphous silica materials. To this end, atomistic details and energetic features can be provided by computer simulation techniques

* Corresponding author. Tel.: +34 91 398 9047; fax: +34 91 398 6697.
*E-mail addresses:* eperez@ccia.uned.es (E. Pérez-Mayoral), esoriano@iqog.csic.es (E. Soriano).

0920-5861/$ – see front matter © 2013 Elsevier B.V. All rights reserved.
http://dx.doi.org/10.1016/j.cattod.2013.10.016

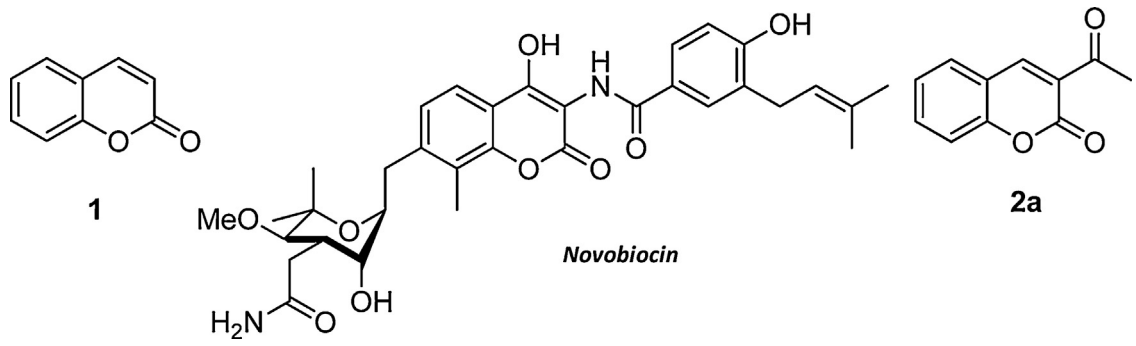


**Fig. 1.** Natural products and biologically active coumarins.

of various kinds, which are becoming essential to get comprehensive views of the interface regions of interest on amorphous silica [16–18]. Different approaches have addressed different topics. In this sense, ab initio periodic calculations (PBC methods) have been successfully performed to obtain insight into the reactivity and other properties (for some examples, see [19–23]). On the other hand, first principles calculations on small size clusters have focused on the spectroscopic properties and reactivity (for some examples, see [24–28]). They allow that standard quantum mechanical methods using highly sophisticated quantum chemistry computer programs can be applied to characterize physicochemical features, energetics, reaction paths, and intermediates. This is a real advantage over the PBC method, because the level of sophistication in the adopted theoretical method is only limited by the available computing resources. However, it is well-known that cluster studies might suffer from edge effect if not used in embedded techniques.

Our most recent contributions in the area of modified mesoporous silicas are addressed to the synthesis of bioactive nitrogen heterocycles or key intermediates through condensation reactions. Thus, we have reported the selective synthesis of quinolones catalyzed by amino-grafted MCM-41 [29] and much more recently the preparation of quinolines by using acid–base bifunctional T/MCF materials (where T is Nb or Al) [30,31], both of them via Friedländer condensation.

1,2-Benzopyrones known as coumarins are a family of naturally occurring oxygen heterocyclic compounds widely distributed in the vegetable kingdom [32]. Everyday humans are continuously exposed to coumarins through the handling of plants and fruit or vegetables ingestion. Coumarins are an important class of oxygen heterocycles which have attracted much attention because of their huge number of applications. This oxygen heterocycle skeleton displays a broad range of biological and pharmacological properties such as analgesic, antimicrobial, vasodilator, anti-inflammatory, antioxidant and anti-cancer and anti-HIV [33]. Additionally, these compounds are considered as important and interesting scaffolds in agrochemical and pharmaceutical industries.

Fig. 1 depicts some natural products and synthetic compounds containing the coumarin skeleton.

Compound **1** is a natural product named coumarin often used in the perfume and cosmetic formulations mainly due to its strong fragrant odor whereas *Novobiocin* is a natural antibiotic. Coumarin **2a** is a synthetic compound useful as building block for the synthesis of 3(substituted)chromen-2-ones, which exhibit antioxidant and anti-inflammatory activities [34].

One of the simplest synthetic approaches to prepare coumarins consists of the condensation of 2-hydroxybenzaldehydes with esters showing enolizable hydrogens at α-position through Knoevenagel condensation, the most useful C=C bond forming strategy in organic synthesis [35]. Although coumarins are widely studied, only a few heterogeneous catalysts showing acid or basic properties have been developed for their synthesis, via Knoevenagel condensation, including heteropolyacids [36], hydrotalcites [37], polystyrene-supported bases [38] and grafted quaternary organic ammonium hydroxides MCM-41 [39].

Our research interest is centered on the design and development of new heterogeneous basic catalysts to promote the synthesis of coumarins from *o*-salicylaldehyde (**3**) and ethyl acetoacetate (**4**) (Scheme 1). In this paper we report the synthesis and characterization of two different amino-grafted mesoporous materials based on SBA-15 structure, as well as their use as catalysts in the synthesis of coumarins under solvent-free and mild conditions. We also studied the influence of the substitution at 5-position over the 2-hydroxybenzaldehydes (**3**) in the condensation reaction. Overall the goal of this paper is the understanding of the reaction mechanism by combining the experimental and computational results herein reported.

## 2. Materials and methods

### 2.1. Synthesis of the catalysts

SBA-15 matrix was synthesized according to the methodology previously reported by Zukal et al. [40].

Amino-grafted SBA-15 materials were synthesized according to the experimental procedure reported in Refs. [41,42] from mesoporous silica SBA-15 and the corresponding trialkoxysilylpropylamine. *In a typical experiment*, to a suspension of dried SBA-15

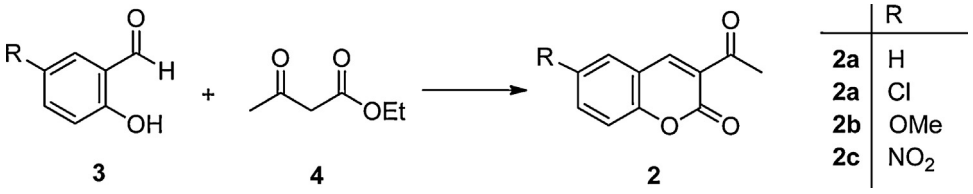


**Scheme 1.** Synthesis of coumarins from 5-substituted 2-hydroxybenzaldehydes (**3**) and ethyl acetoacetate (**4**).

**Table 1**
Textural characteristics and chemical composition for mesoporous silica SBA-15.

| Catalyst | $S_{BET}$ ($m^2$/g) | $D^a$ (Å) | $V^a$ ($cm^3$/g) | $C^b$ [mmol/g] | $N^b$ [mmol/g] |
|---|---|---|---|---|---|
| SBA-15 | 834 | 63 | 0.97 | – | – |
| MAP/SBA-15 | 370 | 56 | 0.68 | 6.64 | 1.53 |
| DEAP/SBA-15 | 388 | 58 | 0.60 | 9.63 | 1.31 |

$S_{BET}$, BET surface area. *D* and *V*, diameter and volume of the pores, respectively.
[a] Determined by BJH method.
[b] Determined by elemental analysis.

(2 g) in toluene (35 mL), 3-methylaminopropyl)trimethoxysilane (6.65 mmol) was added and the mixture was stirred for 5 h at room temperature (296 K). Then, toluene was filtered off and the modified SBA-15 was washed out three times with toluene (20 mL). Finally, the solid was dried in vacuum at room temperature.

The following notation was used for the materials under study: MAP/SBA-15 and DEAP/SBA-15 stand for the silica SBA-15 functionalized with 3-(methylaminopropyl)trimethoxysilane and 3-(diethylamino)propyltrimethoxysilane, respectively.

### 2.2. Characterization of SBA-15 materials

#### 2.2.1. Nitrogen adsorption

Textural parameters of the SBA-15 materials were determined by nitrogen adsorption. Adsorption isotherms of nitrogen at 77 K on molecular sieves under study were recorded using a static volumetric apparatus ASAP 2020 (Micromeritics). In order to attain a sufficient accuracy in the accumulation of the adsorption data, this instrument is equipped with pressure transducers covering the 133 Pa and 133 kPa ranges. Before each sorption measurement the samples were outgassed at 383–393 K overnight until the residual pressure was lower than 0.7 Pa. Table 1 lists some characterization data of the catalysts under study.

#### 2.2.2. Thermal stability

Thermal stability of the solids based on SBA-15 structure was investigated by TG experiments using a TA Instrument SDT Q600.

#### 2.2.3. X-ray diffraction (XRD)

The structure of SBA-15 was confirmed by X-ray powder diffraction with a Seifert C-3000 diffractometer with filtered Cu-Kα radiation in the Bragg-Brentano geometry operating at 40 kV and 30 mA, over powder sample. X-ray powder diffraction pattern of SBA-15 material provided clear evidence of their hexagonal structure and phase purity of sample.

#### 2.2.4. Elemental analyses

Chemical composition of amino-grafted mesoporous silicas was investigated by elemental analyses using an Elementar Analyser Vario EL III instrument.

### 2.3. Catalytic performance

#### 2.3.1. General

NMR spectra were recorded with a Bruker AVANCE DPX-300 (300 MHz for $^1$H). $^1$H chemical shifts (δ) in $CDCl_3$ are given from internal tetramethylsilane.

TLC chromatography was performed on DC-Aulofolien/Kieselgel 60 F245 (Merck).

All reagents and solvents were purchased from Aldrich and Alfa-Aesar.

#### 2.3.2. Experimental procedure

*In a typical procedure*, the catalyst (50 mg) was added to a solution of the 2-hydroxibenzaldehyde (**3a**) (2 mmol) and ethyl acetoacetate (**4**) (2 or 4 mmol), at 323 K, and the reaction mixture was stirred during the appropriated time. After cooling, AcOEt (2 mL) was added to the reaction crude and the catalyst was filtered off and the solvent evaporated in vacuo.

Reactions were followed by TLC using mixtures of hexane/AcOEt as eluents and the products were characterized by $^1$H NMR.

Conversion to coumarins **2** was determined by $^1$H NMR.

### 2.4. Theoretical calculations

Herein, we have performed a theoretical study on the first step of the Knoevenagel condensation, in which the coupling of reactants take place, by the use of finite cluster calculations rather than periodic calculations in order to get more reliable structural information on the interaction between reagents and energetic values at the catalytic sites. This methodology allows to increase the level of calculation and also to have access to broader selection methods. Calculations were performed with Gaussian09 [43]. All geometries [44] were optimized by using the B3LYP functional [45] combined with the 6-31G(d,p) basis set. The stationary points thus obtained were characterized by means of harmonic analysis, and for all the transition structures, the normal mode related to the imaginary frequency corresponds to the nuclear motion along the reaction coordinate under study. The vibrational zero-point and thermal corrections to the thermodynamic results were taken from the frequency calculations. Single-point calculations were performed on the B3LYP geometries with M06/6-311G(2d,p) [46]. NPA charges were computed using the natural bond orbital (NBO) method [47].

## 3. Results and discussion

### 3.1. Synthesis and characterization of the catalysts

We prepared two amino-functionalized mesoporous silicas based on the SBA-15 structure with different basic properties; MAP/SBA-15 and DEAP/SBA-15 containing secondary and tertiary aminopropyl groups, respectively. The mesoporous silica SBA-15, previously synthesized, was activated using a post-synthetic approach by grafting with the corresponding trialkoxysilylpropylamine [42].

Amino-grafted SBA-15 materials showed a considerable decreased specific surface area, $S_{BET}$, regarding the SBA-15 matrix, as expected. However, small differences on textural parameters were observed for MAP/SBA-15 and DEAP/SBA-15; it could be firstly attributed to the slightly lower N loading but also to the highest C content for the DEAP/SBA-15 sample. Furthermore, the slightly decreasing deviation of $S_{BET}$ and pore diameter observed for MAP/SBA-15 could be due to the interaction of the nearest —NHMe groups by hydrogen bonding or even with the silanol groups exhibiting a weak acidic properties [48]. This type of interactions is totally inhibited in DEAP/SBA-15 because of the absence of the —NH protons.

Thermal stability of the samples was investigated by thermogravimetic studies; amino-grafted mesoporous silicas reported herein are stable in a temperature range from room temperature to approximately 453 K.

XRD diffractogram for SBA-15 matrix showed a well-resolved diffraction lines at low angles evidencing the hexagonal structure of the sample.

### 3.2. Catalytic performance

At first, mesoporous silicas reported above were tested in the synthesis of coumarin **2a** from 2-hydroxibenzaldehyde (**3a**) and ethyl acetoacetate (**4**), at 323 K, under solvent-free conditions (Scheme 1).

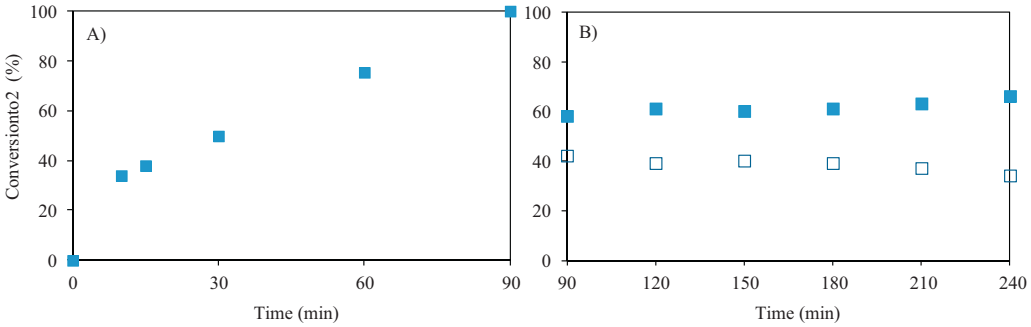


**Fig. 2.** Synthesis of coumarin **2a** from 2-hydroxibenzaldehyde (**3a**) and ethyl acetoacetate (**4**). Reaction conditions: 2-hydroxibenzaldehyde (**3a**) (2 mmol) and ethyl acetoacetate (**4**) (2 mmol) and catalyst (50 mg), at 323 K. (A) Conversion to **2a** determined by GC using mesytilene as internal standard. (B) Conversion to **2a** determined by $^1$H NMR (■) coumarin **2a** and (□) compound **5**.

Fig. 2A depicts a plot of conversion to **2a** versus time for the reaction catalyzed by MAP/SBA-15. We can observe that coumarin **2a** was obtained in quantitative yield after 90 min of reaction time. However, the analysis of the reaction sample by $^1$H NMR showed the presence of a mixture of coumarin **2a** and other reaction product in ratio 3:2. Besides the signals corresponding to coumarin **2a**, the $^1$H NMR spectrum of the sample showed the signals at $\delta$ 7.56 (s), 4.30 (m) and 1.37 (t) which were assigned to CH=C and the ethyl carboxylic ester group accompanying to other proton signals in the aromatic region and the $CH_3$ group at 1.98 ppm.

On the other hand, it was observed the slow transformation of that new reaction product, in the presence of the catalyst, into the compound **2a** (Fig. 2B). It is important to note that the mixture of both products was transformed into the coumarin **2a** on standing, compound **2a** being isolated then as totally pure sample.

Therefore, these results suggest that the reaction of benzaldehyde **3a** and compound **4** takes place by Knoevenegel condensation leading to compound **5a** as intermediate product, which undergoes a lactonization reaction giving the corresponding coumarin **2a** (Scheme 2). Remarkably, while the first step of the reaction is a catalytic process, the intramolecular esterification in compound **5a** would take place in the absence of any catalyst under thermal activation or even at room temperature.

In contrast, mesoporous silica loaded with tertiary amino groups, DEAP/SBA-15, under the same experimental conditions, exclusively yielded coumarin **2a** in only 7% after 2 h of reaction time. These results are in accordance with those reported by Lanari et al. [38].

We also performed the catalytic experiment about the amount of MAP/SBA-15 able to catalyze the reaction between compounds **3a** and **4**. We observed that the reaction takes place in the same degree even in the presence of decreased amounts of the catalyst (25 mg). Additionally, it was observed that mesoporous silica MAP/SBA-15 was a totally recyclable catalyst during at least three times without any activity loss.

In order to explain the observed reactivity, we performed a computational study of the catalytic step of the reaction, the formation of the C—C bond by Knoevenagel condensation between benzaldehyde **3a** and compound **4**. We used the most reduced models of the catalysts including exclusively the basic active sites as shown in Chart 1. This model was selected as it is the minimal structure that contains the key amine, supported on the small silica cluster. While this does not reflect a realistic situation, the model should allow us to get insights into the role of the amine and its implications in these catalytic processes. The optimized structures for this step reveal that the initial reactant complex (**Rc**) is formed by the catalyst, carbonylic acceptor salicylaldehyde (**3a**) and ethyl acetoacetate (**4**) where the molecules interact each other through intermolecular H-bonds (Chart 1) [49].

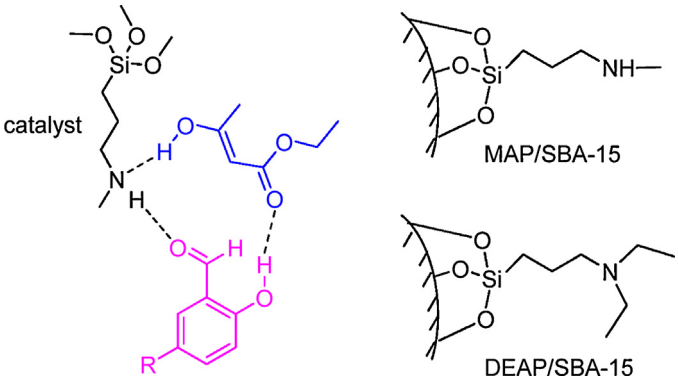


**Chart 1.** Reactant complex, **Rc**. Salicylaldehyde (**3a**) and ethyl acetoacetate (**4**) are colored in pink and blue, respectively. The schematic model of the two amino-functionalized mesoporous silicas based on the SBA-15, MAP/SBA-15 and DEAP/SBA-15, are also depicted. (For interpretation of the references to color in text, the reader is referred to the web version of the article.)

The transition structure (**TS**) computed for the MAP/SBA-15 catalyzed step (Fig. 3) indicates that the C—C bond is forming (2.07 Å), whereas the amine proton is being transferred to the aldehyde (1.34 Å) thus assisting the incipient formation of alcohol. Additionally, the enol proton is mostly transferred to the catalyst, as the distance suggests (1.98 Å). The transition structure drives to the aldol intermediate (**Int**) where the C—C is fully formed and the aldol

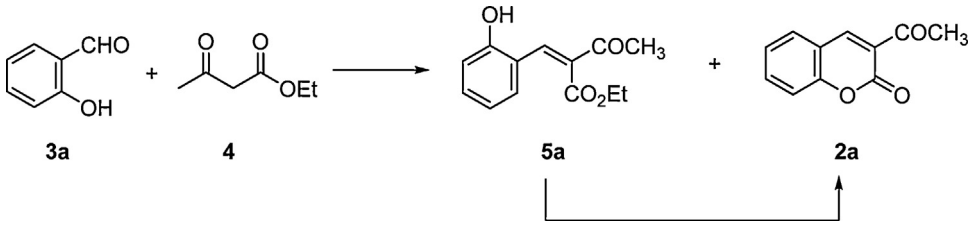


**Scheme 2.** Synthesis of coumarin **2a**.

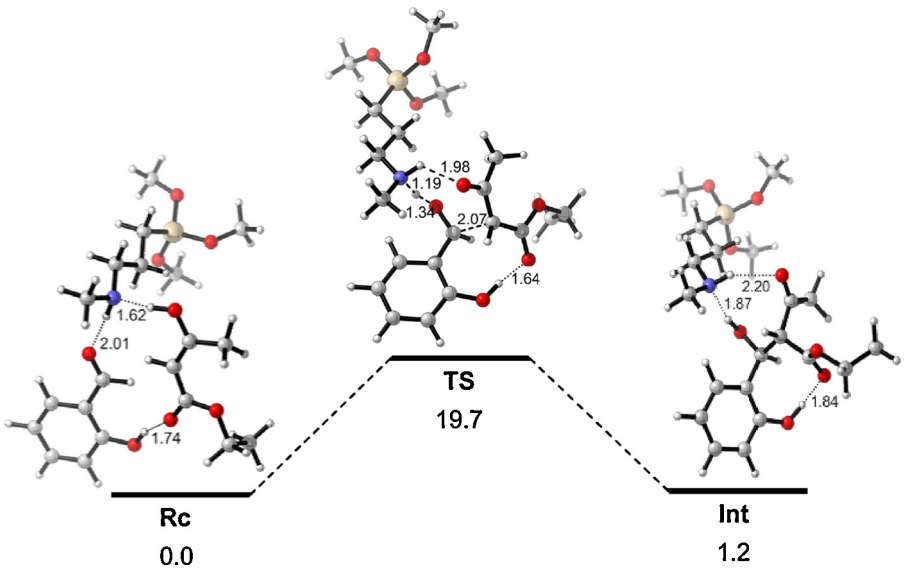


**Fig. 3.** Optimized structures along the C—C bond forming step catalyzed by a model of MAP/SBA-15. Free-energy values relative to **Rc** are shown in kcal/mol.

is doubly H-bonded to the amine group, which acts as an H-donor and H-acceptor (Fig. 3).

As can be observed in Fig. 3, the H-bonding interactions between both the phenolic and the carboxylic group in the aldol intermediate **(Int)** could represent the stabilization force which influence the exclusive formation of the intermediate compound **5a** by dehydration.

A comparison between the C—C bond forming step catalyzed by MAP/SBA-15 and DEAP/SBA-15 provides significant differences. The transition structure computed for the MAP/SBA-15 catalyzed step (Fig. 4 left) indicates that the C—C bond is forming, whereas the ammonium proton is transferred to the aldehyde (1.34 Å) thus assisting the incipient formation of alcohol, as has been described above. Additionally, the enol has mostly transferred the proton to the amine, as the distance in **TS** suggests (1.98 Å) thus regenerating the catalyst and the H-bonded carbonylic group in the subsequent aldol intermediate (**Int**). In the case of the catalyst bearing a tertiary amine group (DEAP/SBA-15, Fig. 4 right), the role of the amine acting as a bifunctional acid–base catalyst is not possible, and the proton of the enolic reagent is partially transferred to the amine and then to the incipient alcohol, to reach the transition structure (as IRC calculations verify).

The computed activation energy values (difference of 11.9 kcal/mol between the two cases) are in accordance with the different reactivity and catalytic activity observed with both basic mesoporous solids.

These results suggest that the amine group in MAP/SBA-15 acts as a dual acid–base catalyst and assists the approaching of the reagents to each other, strongly stabilizing the transition structure.

In addition, we have studied the influence of the substitution in the 2-hydroxybenzaldehydes (**3**) at 5-position in the synthesis of coumarins **2**. In this sense, we compared the results for the synthesis of coumarins **2** starting from salicylaldehydes **3b** (R = Cl) and **3c** (R = OMe), with substituents exhibiting different electronic properties, catalyzed by MAP/SBA-15 under the same experimental conditions above mentioned. The conversion to the corresponding coumarin **2b** or **2c** and the intermediate products **5b** or **5c** is shown in Fig. 5.

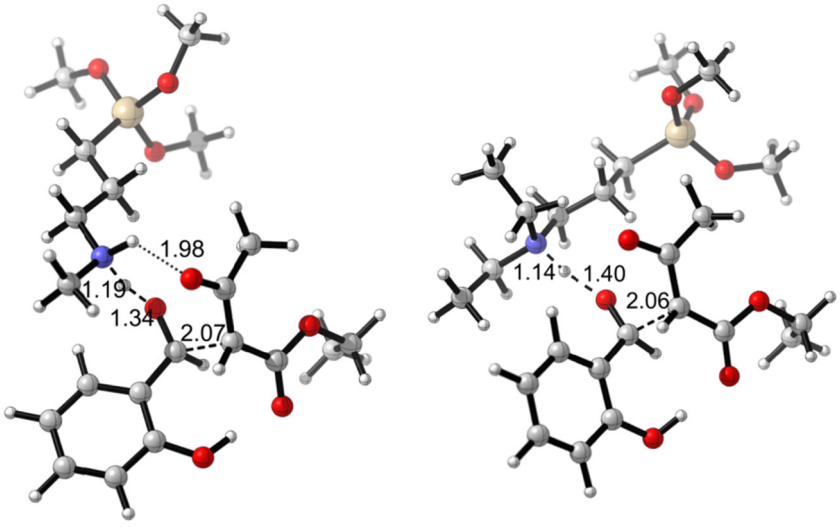


**Fig. 4.** Transition structure for the C—C bond forming step catalyzed by MAP/SBA-15 (left) and DEAP/SBA-15 (right). Some relevant distances are shown in Å.

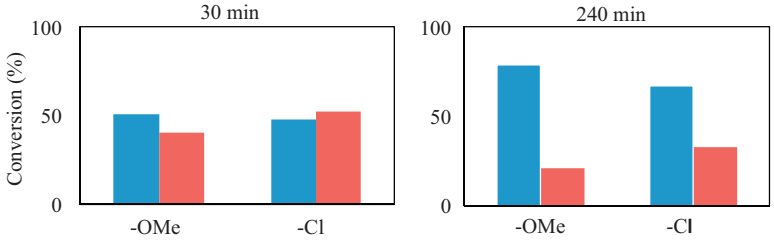


**Fig. 5.** Synthesis of coumarins **2b**, **c** from salicylaldehydes **3b**, **c** and ethyl acetoacetate (**4**); coumarins **2** are shown in blue and compounds **5** are in red. Reaction conditions: 2-hydroxybenzaldehydes (**3b** or **3c**) (2 mmol) and ethyl acetoacetate (**4**) (2 mmol) and catalyst (50 mg), at 323 K. (For interpretation of the references to color in text, the reader is referred to the web version of the article.)

**Table 2**
Free-energy barrier (in kcal/mol), NPA charge at the carbonylic carbon of **3** on the **Rc** complex, and relevant distances in the transition structure, **TS** (in Å).

| Catalyst | *R* | $\Delta G^{\#}$ (kcal/mol) | NPA charge at C-acceptor in Rc | H. . .O distance between 3 and 4 in TS | C—C distance (Å) in TS |
|---|---|---|---|---|---|
| MAP/SBA15 | H | 19.7 | 0.4601 | 1.639 | 2.069 |
| | OMe | 17.0 | 0.4677 | 1.661 | 2.051 |
| | Cl | 20.6 | 0.4614 | 1.635 | 2.029 |
| | $NO_2$ | 24.1 | 0.4594 | 1.592 | 2.004 |

From Fig. 5, we can observe that in both cases the conversion to products is almost total after only 30 min of reaction time, selectivity to coumarin **2c** (R = OMe, 56%) being higher than to **2b** (R = Cl, 48%). This feature is emphasized at the highest reaction times; selectivity to **2c** was 79% whereas that for **2b** was significantly lowers (67%). Then, these results clearly indicate that the presence of substituents with different electronic properties at 5-position have effects not only on the acceptor capability of —CHO group but also over the acidity or nucleophility of —OH group in benzaldehydes **3b-c**.

We also carried out the reaction of salicylaldehyde **3d** possessing a strong electro-withdrawing moiety, $-NO_2$, and ethyl acetoacetate (**4**) in the presence of MAP/SBA-15 (Fig. 6). In this case, we performed the condensation at higher temperature, 353 K, because of the lower reactivity of the corresponding benzaldehyde **3d**.

As depicted in Fig. 6, compound **3d** is quantitatively converted into coumarin **2d** and compound **5d** in 40 and 60% of chemical yield, respectively, in only 15 min of reaction time. In this case, it was observed the progressive transformation of **5d** to **2d**, which was isolated as totally pure sample after 4 h of reaction time.

In order to address the effect of the aromatic substituents, we have performed calculations on the 2-hydroxy-5-sustituted benzaldehydes under study. The optimized transition structures are shown in Fig. 7 and the computed barriers are summarized in Table 2. As can be deduced from Fig. 7, the substituent does not involve further interactions (such as H-bond) with the catalyst, so its effect is electronic in nature.

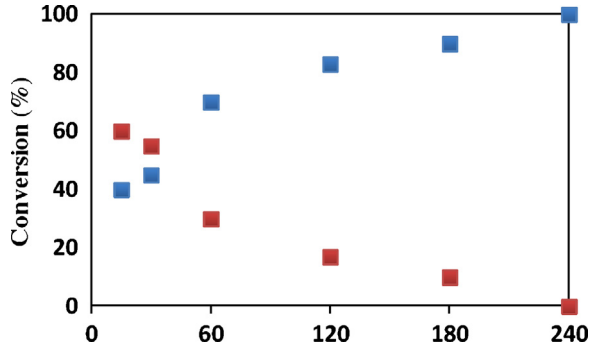


**Fig. 6.** Synthesis of coumarin **2d** from benzaldehyde **3d** and ethyl acetoacetate (**4**). Coumarin **3d** is shown in blue and compound **5d** in red. Reaction conditions: 2-hydroxibenzaldehyde (**3d**) (2 mmol) and ethyl acetoacetate (**4**) (2 mmol) and catalyst (50 mg), at 353 K. (For interpretation of the references to color in text, the reader is referred to the web version of the article.)

The results reveal that the C—C forming bond for R = —OMe proceeds with the lowest free-energy (and enthalpy, not shown) barrier, whereas the step is kinetically less favored when R = —Cl and $-NO_2$. In fact, the presence of this strong electro-withdrawing group leads to the highest barrier for the formation of the aldol as expected. The inverse order is (surprisingly) followed by the

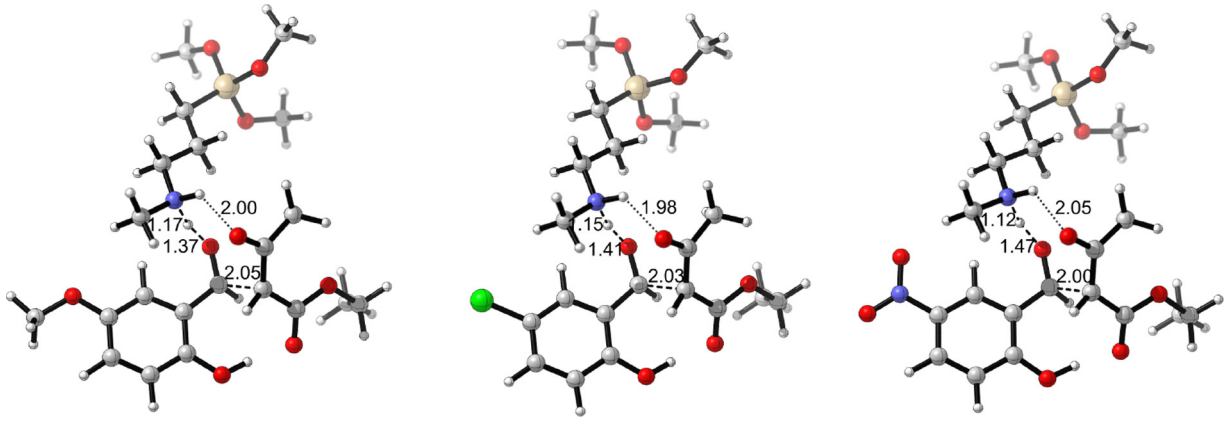


**Fig. 7.** Transition structures for 2-hydroxybenzaldehydes bearing substituents with different nature at 5-position (R = —OMe, left; R = —Cl, middle; R = —$NO_2$, right). Some relevant distances are shown in Å.

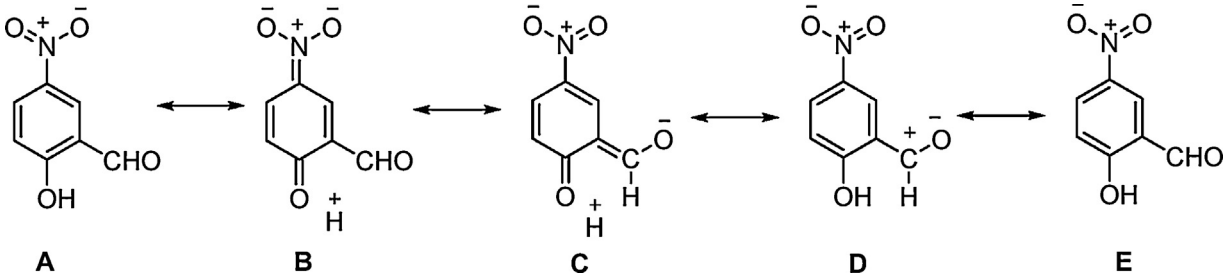


**Chart 2.** Resonance forms for the 5-$NO_2$ substituted salicylaldehyde.

calculated NPA charge on the acceptor carbonylic carbon of the initial reactant complex (**Rc**), as the electro-donor —OMe group increases the NPA charge (electrophilicity) of the aldehyde whereas the electro-withdrawal group —$NO_2$ reduces it. This unexpected effect can be attributed to a more acute effect of the 5-substituent on the *para*-position (OH group), i.e., the impact of resonance forms **B** and **C** (Chart 2) for the 5-$NO_2$ substituted aldehyde, for instance. In this sense, the structure bearing a 5-$NO_2$ group shows a more acidic OH group, as the short distance (strong H-bond) with the carbonyl moiety of **4** on the transition structure suggests. The opposite is true for the 5-OMe substituted structure (higher NPA charge and longer H-bond with **4** in **TS**).

Overall, the results suggest that the substituent at the 5-position has two electronic effects: (a) on the acidity of the *para*-OH group, and (b) on the eletrophilicity of the carbonyl acceptor. For electron-withdrawal groups, the former should stabilize the reactant complex (**Rc**), while the latter should disfavor the coupling, hence both effects increasing the activation barrier.

The coupling step is weakly exergonic for the studied salicylaldehydes (−0.2 to −1.6 kcal/mol).

## 4. Conclusions

We report on the first amino-grafted mesoporous silica loaded with secondary amine groups, MAP/SBA-15, which efficiently catalyzes the synthesis of coumarins from ethyl acetoacetate (**4**) and 2-hydroxybenzaldehydes (**3**) under solvent-free and mild conditions.

The reaction is proposed to proceed through Knoevenagel condensation between reagents and subsequent non-catalyzed lactonization of the corresponding intermediate species.

The experimental and theoretical results reported herein demonstrate that the amine group nature in amino-grafted SBA-15 materials is a determining factor in the reaction course. In this sense, DEAP/SBA-15 containing tertiary amine groups is a less active catalyst for the synthesis of coumarins than its analog loaded with methylaminopropyl groups. Besides the unfavorable steric effects of ethyl groups in DEAP/SBA-15, the different catalytic activity is mainly due to the presence of —NH proton which strongly stabilizes the transition structure for MAP/SBA-15. In this sense, our theoretical results suggest that the secondary amine group in MAP/SBA-15 acts as dual acid–base catalysts favoring the approaching of the reagents to each other and then strongly stabilizing the transition structure.

Finally, the presence of the substituents at 5-position in 2-hydroxybenzaldehydes (**3**) shows a key role in the electrophilic character of the carbonyl group and also in the acidity of phenolic group, which accounts for the observed reactivity.

## Acknowledgements

This work has been supported by MICINN (projects CTQ2009-10478 and CTQ2011-27935). We are grateful to the Centro de Supercomputación de Galicia (CESGA) for generous allocation of computing resources.

## References

[1] J.S. Beck, J.C. Vartuli, W.J. Roth, M.E. Leonowicz, C.T. Kresge, K.D. Schmitt, C.T.W. Chu, D.H. Olson, E.W. Sheppard, S.B. McCullen, J.B. Higgins, J.L. Schlenker, J. Am. Chem. Soc. 114 (1992) 10834–110834.
[2] F. Hoffmann, M. Cornelius, J. Morell, M. Fröba, Angew. Chem. Int. Ed. 45 (2006) 3216–3251.
[3] F.-Y. Changa, K.-J. Chao, H.-H. Cheng, C.-S. Tan, Sep. Purif. Technol. 70 (2009) 87–95.
[4] S.-N. Kim, W.-J. Son, J.-S. Choi, W.-S. Ahn, Micropor. Mesopor. Mater. 115 (2008) 497–503.
[5] H.Y. Huang, R.T. Yang, D. Chinn, C.L. Munson, Ind. Eng. Chem. Res. 42 (2003) 2427–2433.
[6] S. Kim, J. Ida, V.V. Guliants, J.Y.S. Lin, J. Phys. Chem. B 109 (2005) 6287–6293.
[7] S. Loganathan, M. Tikmani, A.K. Ghoshal, Langmuir 29 (2013) 3491–3499.
[8] A. Olea, E.S. Sanz-Pérez, A. Arencibia, R. Sanz, G. Calleja, Adsorption 19 (2013) 589–600.
[9] N. Hiyoshi, K. Yogo, T. Yashima, Micropor. Mesopor. Mater. 84 (2005) 357–365.
[10] N. Hiyoshi, K. Yogo, T. Yashima, Chem. Lett. 33 (2004) 510–511.
[11] X. Feng, G. Hu, X. Hu, G. Xie, Y. Xie, J. Lu, M. Luo, Ind. Eng. Chem. Res. 52 (2013) 4221–4228.
[12] I. Matos, E. Pérez-Mayoral, E. Soriano, A. Zukal, R.M. Martín-Aranda, A.J. López-Peinado, I. Fonseca, J. Cejka, Chem. Eng. J. 161 (2010) 377–383.
[13] I. Sobczak, M. Ziolek, E. Pérez-Mayoral, D. Blasco-Jiménez, A.J. López-Peinado, R.M. Martín-Aranda, Catal. Today 179 (2012) 159–163.
[14] D. Blasco-Jiménez, I. Sobczak, M. Ziolek, A.J. López-Peinado, R.M. Martín-Aranda, Catal. Today 152 (2010) 119–125.
[15] D. Blasco-Jiménez, A.J. López-Peinado, R.M. Martín-Aranda, M. Ziolek, I. Sobczak, Catal. Today 142 (2009) 283–287.
[16] A. Rimola, D. Costa, M. Sodupe, J.-F. Lambert, P. Ugliengo, Chem. Rev. 113 (2013) 4216–4313.
[17] F. Tielens, C. Gervais, J.-F. Lambert, F. Mauri, D. Costa, Chem. Mater. 20 (2008) 3336–3344.
[18] P. Ugliengo, M. Sodupe, F. Musso, I.J. Bush, R. Orlando, R. Dovesi, Adv. Mater. 20 (2008) 4579–4583.
[19] Y.L. Zhao, S. Koppen, T. Frauenheim, J. Phys. Chem. C 115 (2011) 9521–9615.
[20] M. Nonella, S. Seeger, Chem. Phys. 378 (2010) 73–81.
[21] A. Rimola, M. Sodupe, P. Ugliengo, J. Phys. Chem. C 113 (2009) 5741–5750.
[22] T.P.M. Goumans, C.R.A. Catlow, W.A. Brown, J. Chem. Phys. 128 (2008) 134709.
[23] H. Guesmi, F. Tielens, J. Phys. Chem. C 116 (2012) 994–1001.
[24] S. Bordiga, I. Roggero, P. Ugliengo, A. Zecchina, V. Bolis, G. Artioli, R. Buzzoni, G. Marra, F. Rivetti, G. Spano, C. Lamberti, J. Chem. Soc. Dalton Trans. 342 (2001) 3921–3929.
[25] V. Bolis, C. Busco, P. Ugliengo, J. Phys. Chem. B 110 (2006) 14849–14859.
[26] C.A. Demmelmaier, R.E. White, J.A. van Bokhoven, S.L. Scott, J. Catal. 262 (2009) 44–56.
[27] J. Handzlik, J. Ogonowski, J. Phys. Chem. C 116 (2012) 5571–5584.
[28] J. Handzlik, R. Grybos, F. Tielens, J. Phys. Chem. C 117 (2013) 8138–8149.
[29] F. Domínguez-Fernández, J. López-Sanz, E. Pérez-Mayoral, D. Bek, R.M. Martín-Aranda, A.J. López-Peinado, J. Cejka, ChemCatChem 1 (2009) 241–243.
[30] A. Smuszkiewicz, E. Pérez-Mayoral, E. Soriano, I. Sobczak, M. Ziolek, R.M. Martín-Aranda, A.J. López-Peinado, Catal. Today (2013), http://dx.doi.org/10.1016/j.cattod.2013.04.034.
[31] A. Smuszkiewicz, J. López-Sanz, E. Pérez-Mayoral, E. Soriano, I. Sobczak, M. Ziolek, R.M. Martín-Aranda, A.J. López-Peinado, J. Mol. Catal. A: Chem. 378 (2013) 38–46.
[32] M.F. Martins Borges, F.M. Fernandes Roleira, N.J. da Silva Pereira Milhazes, E. Uriarte Villares, L. Santana Penin, Front. Med. Chem. 4 (2009) 23–85.
[33] K.M. Paramjeet, S. Dipak, D. Arti, J. Chem. Pharm. Res. 4 (2012) 822–850.
[34] B. Lakshmi Narayanan, L.A. Pradeep Rajkumar, A. Arulanandham, N. Satheesh Babu, T. Gayathri, A. Raju, Int. J. Pharm. Sci. Res. 3 (2012) 474–478.
[35] Y.F. Han, M. Xia, Curr. Org. Chem. 14 (2010) 379–413.
[36] M.M. Heravi, S. Sadjadi, H.A. Oskooie, R.H. Shoar, F.F. Bamoharram, Catal. Commun. 9 (2008) 470–474.
[37] A. Ramani, B.M. Chanda, S. Velu, S. Sivasanker, Green Chem. 1 (1999) 163–165.

[38] D. Lanari, R. Ballini, A. Palmieri, F. Pizzo, L. Vaccaro, Eur. J. Org. Chem. (2011) 2874–2884.
[39] I. Rodriguez, S. Iborra, F. Rey, A. Corma, Appl. Catal. A: Gen. 194–195 (2000) 241–252.
[40] A. Zukal, H. Siklová, J. Cejka, Langmuir 24 (2008) 9837–9842.
[41] H. Balcar, J. Cejka, J. Sedlacek, J. Svoboda, J. Zednik, Z. Bastl, V. Bosacek, J. Vohlidal, J. Mol. Catal. A 203 (2003) 287–298.
[42] J. Lopez-Sanz, E. Pérez-Mayoral, E. Soriano, M. Sturm, R.M. Martín-Aranda, A.J. Lopez-Peinado, J. Cejka, Catal. Today 187 (2012) 97–103.
[43] M.J. Frisch, G.W. Trucks, H.B. Schlegel, G.E. Scuseria, M.A. Robb, J.R. Cheeseman, G. Scalmani, V. Barone, B. Mennucci, G.A. Petersson, H. Nakatsuji, M. Caricato, X. Li, H.P. Hratchian, A.F. Izmaylov, J. Bloino, G. Zheng, J.L. Sonnenberg, M. Hada, M. Ehara, K. Toyota, R. Fukuda, J. Hasegawa, M. Ishida, T. Nakajima, Y. Honda, O. Kitao, H. Nakai, T. Vreven, J.A. Montgomery Jr., J.E. Peralta, F. Ogliaro, M. Bearpark, Heyd J.J., E. Brothers, K.N. Kudin, V.N. Staroverov, T. Keith, R. Kobayashi, J. Normand, K. Raghavachari, A. Rendell, J.C. Burant, S.S. Iyengar, J. Tomasi, M. Cossi, N. Rega, J.M. Millam, M. Klene, J.E. Knox, J.B. Cross, V. Bakken, C. Adamo, J. Jaramillo, R. Gomperts, R.E. Stratmann, O. Yazyev, A.J. Austin, R. Cammi, C. Pomelli, J.W. Ochterski, R.L. Martin, K. Morokuma, V.G. Zakrzewski, G.A. Voth, P. Salvador, J.J. Dannenberg, S. Dapprich, A.D. Daniels, O. Farkas, J.B. Foresman, J.V. Ortiz, J. Cioslowski, D.J. Fox, Gaussian 09, Revision B01, Gaussian Inc, Wallingford, CT, 2010.
[44] C.Y. Legault, CYLview, 1.0b, Université de Sherbrooke, 2009.
[45] (a) A.D. Becke, J. Chem. Phys. 98 (1993) 5648–5652;
(b) C. Lee, W. Yang, R.G. Parr, Phys. Rev. B 37 (1988) 785–789.
[46] Y. Zhao, D.G. Truhlar, Theor. Chem. Acc. 120 (2008) 215–241.
[47] E.D. Glendening, A.E. Reed, J.E. Carpenter, F. Weinhold, NBO Version 3.1.
[48] M.W. McKittrick, C.W. Jones, Chem. Mater. 15 (2003) 1132–1139.
[49] Several plausible reactant complexes in which the catalytic amine and reactants were H-bonded to each other, were studied. This assumption was made on the base of chemical intuition, in turn supported by the computed electrostatic potential maps on the reagents and amine. Additionally, the model selected showed the less congested structure, thus allowing the achievement of a more stable transition structure than from alternative crowded reactant complexes, without severe steric strain.